Journal of Physiology (1993), **465**, *pp.* 359–386
With 11 *figures*
Printed in Great Britain

CALCIUM RELEASE-ACTIVATED CALCIUM CURRENT IN RAT MAST CELLS

BY MARKUS HOTH AND REINHOLD PENNER

From the Department of Membrane Biophysics, Max-Planck-Institute for Biophysical Chemistry, Am Fassberg, D-3400 Göttingen, Germany

(*Received 17 July 1992*)

SUMMARY

1. Whole-cell patch clamp recordings of membrane currents and fura-2 measurements of free intracellular calcium concentration ($[Ca^{2+}]_i$) were used to study the biophysical properties of a calcium current activated by depletion of intracellular calcium stores in rat peritoneal mast cells.

2. Calcium influx through an inward calcium release-activated calcium current (I_{CRAC}) was induced by three independent mechanisms that result in store depletion: intracellular infusion of inositol 1,4,5-trisphosphate ($InsP_3$) or extracellular application of ionomycin (active depletion), and intracellular infusion of calcium chelators (ethylene glycol bis-*N*,*N*,*N*′,*N*′-tetraacetic acid (EGTA) or 1,2-bis(2-aminophenoxy)ethane-*N*,*N*,*N*′,*N*′-tetraacetic acid (BAPTA)) to prevent reuptake of leaked-out calcium into the stores (passive depletion).

3. The activation of I_{CRAC} induced by active store depletion has a short delay (4–14 s) following intracellular infusion of $InsP_3$ or extracellular application of ionomycin. It has a monoexponential time course with a time constant of 20–30 s and, depending on the complementary Ca^{2+} buffer, a mean normalized amplitude (at 0 mV) of 0·6 pA pF^{-1} (with EGTA) and 1·1 pA pF^{-1} (with BAPTA).

4. After full activation of I_{CRAC} by $InsP_3$ in the presence of EGTA (10 mM), hyperpolarizing pulses to −100 mV induced an instantaneous inward current that decayed by 64% within 50 ms. This inactivation is probably mediated by $[Ca^{2+}]_i$, since the decrease of inward current in the presence of the fast Ca^{2+} buffer BAPTA (10 mM) was only 30%.

5. The amplitude of I_{CRAC} was dependent on the extracellular Ca^{2+} concentration with an apparent dissociation constant (K_D) of 3·3 mM. Inward currents were non-saturating up to −200 mV.

6. The selectivity of I_{CRAC} for Ca^{2+} was assessed by using fura-2 as the dominant intracellular buffer (at a concentration of 2 mM) and relating the absolute changes in the calcium-sensitive fluorescence (390 nm excitation) with the calcium current integral. This relationship was almost identical to the one determined for Ca^{2+} influx through voltage-activated calcium currents in chromaffin cells, suggesting a similar selectivity. Replacing Na^+ and K^+ by *N*-methyl-D-glucamine (with Ca^{2+} ions as exclusive charge carriers) reduced the amplitude of I_{CRAC} by only 9% further suggesting a high specificity for Ca^{2+} ions.

MS 1625

7. The current amplitude was not greatly affected by variations of external Mg^{2+} in the range of 0–12 mM. Even at 12 mM Mg^{2+} the current amplitude was reduced by only 23%.

8. I_{CRAC} was dose-dependently inhibited by Cd^{2+}. The concentration–response relationship for Cd^{2+} could be described by a Michaelis–Menten function with an apparent K_D of 0·24 mM and a Hill coefficient of 1.

9. All other tested divalent ions also dose-dependently and reversibly inhibited I_{CRAC}. The order of potency was determined by the relative blocking efficacy of 1 mM of the respective ions: $Ba^{2+} \approx Sr^{2+} < Ni^{2+} < Mn^{2+} \approx Co^{2+} \approx Be^{2+} < Cd^{2+} < Zn^{2+}$. The trivalent ion La^{3+} was the most potent blocker of I_{CRAC}.

10. I_{CRAC} excluded monovalent ions in the presence of divalent ions. Complete removal of divalent ions typically resulted in a triphasic conductance change: an initial decrease in the calcium current, an abrupt increase in inward current with modest inward rectification due to passage of monovalent ions, and a subsequent decrease in total current with a linear current–voltage relationship. At the same time, these changes were accompanied by a shift in the reversal potential from $> +50$ to 0 mV.

11. While all the features of I_{CRAC} are compatible with an ion channel mechanism, there was no significant increase in current noise associated with its activation.

12. Our results suggest that the calcium current activated by depletion of intracellular calcium stores is a highly selective pathway for calcium entry into mast cells and may constitute one of the mechanisms underlying the plateau phase of elevated cytosolic calcium concentration following receptor-mediated release of intracellular calcium.

INTRODUCTION

An increase in free intracellular Ca^{2+} concentration $[Ca^{2+}]_i$ is a ubiquitous mechanism by which cells control a variety of their functions. The rise in $[Ca^{2+}]_i$ can occur either by release of calcium from internal stores or by influx of external calcium across the plasma membrane (Putney, 1990; Irvine, 1990; Meldolesi, Clementi, Fasolato, Zacchetti & Pozzan, 1991). In many cell types the increase in $[Ca^{2+}]_i$ is due to both calcium release and calcium influx. The observed changes in $[Ca^{2+}]_i$ in response to a calcium-mobilizing agonist are typically composed of a transient calcium spike due to Ca^{2+} release and a more prolonged plateau phase of elevated $[Ca^{2+}]_i$ that critically depends on the presence of external calcium and thus is due to Ca^{2+} entry across the plasma membrane.

While the mechanism of receptor-mediated calcium release generally can be attributed to the actions of the second messenger inositol 1,4,5-trisphosphate ($InsP_3$), the instruments of calcium influx in electrically non-excitable cells appear to be rather diverse (Berridge & Irvine, 1989; Sage, 1992). In some cases the agonist itself may gate ion channels permeable to calcium; in others, intracellular messengers generated by the agonist can serve this function (Meldolesi & Pozzan, 1987; Penner, Matthews & Neher, 1988; Matthews, Neher & Penner, 1989*a*; Mahaut-Smith, Sage & Rink, 1992). In most cases, these ion channels only poorly discriminate between mono- and divalent cations. Therefore, these currents are mainly carried by monovalent Na^+ ions and their amplitudes have to be large in order to account for

changes in $[Ca^{2+}]_i$. In many cells, however, inward currents are not readily detectable, despite the registration of calcium entry by calcium-sensitive dyes (Meldolesi *et al.* 1991). This may be due to alternative, more selective calcium influx mechanisms that do not carry sizeable current.

As evident from a number of investigations, the regulation of Ca^{2+} entry is tightly linked to the filling state of intracellular calcium stores (Putney, 1990; Irvine, 1990). The mere depletion of internal Ca^{2+} stores seems to activate Ca^{2+} influx by an as yet unidentified signal transmitted from the organelles to the plasma membrane. Recently, we described the presence of a Ca^{2+} current in mast cells that can be activated by depletion of internal calcium stores (Hoth & Penner, 1992). We have termed this current I_{CRAC} (for calcium release-activated calcium), since the release of Ca^{2+} from intracellular stores by three independent mechanisms activated the same characteristic Ca^{2+} conductance. This current can be measured under favourable conditions where extracellular Ca^{2+} is high (10 mM) and intracellular Ca^{2+} is buffered to low levels by EGTA or BAPTA (10 mM).

In this study, we characterize the biophysical properties of the calcium release-activated calcium current I_{CRAC} in rat peritoneal mast cells. This study is based on the analysis of more than 700 single-cell experiments and provides data about the activation kinetics, the ionic selectivity, and the blocking effects of divalent metal ions. These indicate that I_{CRAC} is a highly specific current that is almost exclusively carried by Ca^{2+} ions. While most features of the current suggested that the conductance change is due to an ion channel mechanism, there was no detectable single-channel activity and no measurable increase in current variance. Since calcium influx following depletion of intracellular calcium stores is recognized as a rather ubiquitous phenomenon, these data should be helpful in identifying and comparing similar calcium influx mechanisms in other cell types.

METHODS

Mast cell purification and culture

Mast cells from rat peritoneum were obtained as described previously (von zur Mühlen, Eckstein & Penner, 1991). Male Wistar rats (200–300 g) were ether-anaesthetized and decapitated. A cell mixture was collected by peritoneal lavage with a Ringer solution containing (mM): NaCl, 140; KCl, 2·8; $CaCl_2$, 2; $MgCl_2$, 2; glucose, 11; Hepes–NaOH, 10; pH 7·2. Subsequently, mast cells were purified to more than 95% homogeneity by Percoll gradient centrifugation at 4 °C for 20 min (34000 *g*). The band containing mast cells was collected and resuspended in Ringer solution of the above composition and briefly centrifuged to obtain a pellet of mast cells. The supernatant was removed and the cells were resuspended in modified medium M199 supplemented with fetal calf serum (10%), $NaHCO_3$ (45 mM), glucose (2·5 mM), streptomycin (0·12 mg ml^{-1}), and penicillin (0·664 mg ml^{-1}). Finally, using this medium, mast cells were co-cultured on glass coverslips with Swiss 3T3 fibroblasts and incubated at 37 °C and 10% CO_2. Cells were used within 1–4 days in which time no obvious changes relevant to the phenomena described in this study were noticed.

For comparison of calcium selectivity of I_{CRAC} with voltage-activated calcium currents, we used bovine adrenal chromaffin cells kept in short-term culture. The purification and culturing conditions for this preparation are described elsewhere (Fenwick, Marty & Neher, 1982*a*).

External and internal solutions

For experiments, coverslips were transferred to the recording chamber and kept in a Ringer solution of the following composition (mM): NaCl, 140; KCl, 2·8; $CaCl_2$, 10; $MgCl_2$, 2; glucose, 11; Hepes–NaOH, 10; pH 7·2. In some experiments the divalent ion concentration of the external

solution was changed as described in the text or figure legends. In experiments where all divalent ions were omitted from the extracellular solution, remaining contaminations were chelated by addition of EGTA or EDTA (1 mM). For selectivity studies, extracellular Na^+ and K^+ in the standard Ringer solution were replaced by *N*-methyl-D-glucamine (142·8 mM). In some experiments active depletion of internal Ca^{2+} stores was induced by extracellularly applied ionomycin (Calbiochem). Ionomycin stock solution (14 mM in dimethyl sulphoxide (DMSO)) was diluted to a final concentration of 14 μM in Ringer solution. External solution changes were made by pressure ejection (10 cmH_2O) from a wide-tipped puffer pipette ($\sim$ 10 μm) positioned about 10–20 μm from the cell under investigation. For recording of voltage-activated Ca^{2+} currents in chromaffin cells, an extracellular solution of the following composition was used (mM): NaCl, 125; KCl, 2·8; $CaCl_2$, 10; $MgCl_2$, 2; tetraethylammonium chloride (TEA), 10; tetrodotoxin (TTX), 0·001; glucose, 11; Hepes–NaOH, 10; pH 7·2.

The standard intracellular solution contained (mM): potassium glutamate, 145; NaCl, 8; $MgCl_2$, 1; Mg-ATP, 0·5; Hepes–KOH, 10; pH 7·2. For recording of voltage-activated Ca^{2+} currents in chromaffin cells, potassium glutamate was replaced by caesium glutamate. Active depletion of intracellular stores was induced by adding InsP_3 (10 μM, Amersham) to the pipette solution. In addition, EGTA or BAPTA (10 mM) were included to increase the driving force for calcium influx, to prevent refilling of the stores, and to reduce calcium-induced inactivation of I_{CRAC}. Fura-2 pentapotassium salt (Molecular Probes, Eugene, OR, USA) was added to the internal solution (100 μM, unless otherwise stated).

Current recording and data analysis

Experiments were performed at room temperature (22–26 °C) in the tight-seal whole-cell configuration of the patch-clamp technique using Sylgard-coated patch pipettes with resistances of 2–5 MΩ. Series resistances were in the range of 5–20 MΩ. High-resolution membrane currents were recorded using an EPC-9 patch-clamp amplifier (HEKA, Lambrecht, Germany) controlled by the 'E9SCREEN' software on an Atari computer. All voltages were corrected for a liquid junction potential of 8 mV between external and internal solutions. High-resolution currents were low-pass filtered at 2·3 kHz and acquired at a sampling rate of 10 kHz, while a charting program on another computer synchronously recorded at low resolution (typically 2 Hz) parameters such as holding potential, holding current (low-pass filtered at 500 Hz), fura-2 fluorescence, and timing of solution changes.

Voltage ramps were of 50 ms duration, covering a range of −100 to +100 mV. In most experiments, thirty voltage ramps were applied immediately after establishment of the whole-cell configuration at maximal stimulation rate (about 1·5 Hz). Capacitance and series resistance were cancelled before each voltage ramp using the automatic neutralization routine of the EPC-9. Subsequent ramps were spaced at 10 s intervals. For analysis, the very first ramps before activation of I_{CRAC} were digitally filtered at 1 kHz, pooled and used for leak subtraction of the subsequent current records.

A holding potential of 0 mV was used throughout this study, because it is close to the zero-current voltage under our experimental conditions and because the electrical driving force for calcium influx at this potential is moderate enough to be coped with by the intracellularly supplied buffers EGTA or BAPTA. For analysis of current amplitudes in some experiments, we have used the values obtained at −40 mV (either from ramp currents or from currents induced by voltage pulses delivered specifically to this potential). The potential of −40 mV was chosen because it is close to the reversal potential of chloride currents and thus minimizes small contaminations introduced by an occasional activation of Cl^- conductances (Penner *et al.* 1988; Matthews, Neher & Penner, 1989*b*).

Variance analysis was performed on-line at a rate of 0·5–1 Hz by sampling 500 ms sections of membrane currents with a sampling rate of 5 kHz and low-pass filtered at 500 Hz (effective bandwidth: 2–500 Hz).

Fluorescence measurements

Measurement of fura-2 fluorescence from single mast cells in the whole-cell configuration was essentially as described elsewhere (Neher, 1989). Cells were loaded with fura-2 by diffusion from the patch pipette and $[Ca^{2+}]_i$ was calculated from the fluorescence ratio at two excitation wavelengths (360/390 nm).

Experiments for estimating calcium fluxes through I_{CRAC} were performed by loading cells with a high concentration of fura-2 (2 mM). Leak currents were determined before activation of I_{CRAC} and used for leak correction of currents induced by applying square voltage pulses to negative membrane potentials (−100 mV). In chromaffin cells, fura-2 was used at 0·5 mM, which is sufficiently high to constitute the dominant buffer in chromaffin cells (Neher & Augustine, 1992), while producing a fluorescence signal comparable to 2 mM fura-2 in mast cells. This may reflect differences in the accessible volume of the two cell types. Voltage-dependent Ca^{2+} currents in chromaffin cells were activated by depolarizing voltage pulses to +10 mV and leak corrected by a P/4 protocol. For comparison of both cell types, leak-corrected current integrals and the absolute changes in the calcium-sensitive fluorescence signal of fura-2 (390 nm excitation wavelength) were used to assess the net calcium flux component of the currents according to

$$R = \frac{\Delta F_{390}}{\int I_{CRAC}\,dt},$$

where R is the ratio, ΔF_{390} is the change in fluorescence at 390 nm, and $\int I_{CRAC}\,dt$ is the integral of the calcium current over the voltage pulse. For details of relating fluorescence changes and Ca^{2+} currents see Neher & Augustine (1992).

RESULTS

Activation of I_{CRAC} by depletion of calcium stores

In a previous publication (Hoth & Penner, 1992), we demonstrated that depletion of intracellular calcium stores by three independent mechanisms (by addition of $InsP_3$, ionomycin or excess of intracellular Ca^{2+} buffers) commonly induces the activation of an inwardly rectifying, voltage-independent calcium current which we termed I_{CRAC}. The activation of this current is demonstrated in Fig. 1*A*, which shows a three-dimensional plot of an experiment in which $InsP_3$ (10 μM) and EGTA (10 mM) were included in the standard pipette solution. Immediately after obtaining the whole-cell configuration, a voltage-ramp protocol was run to obtain instantaneous current–voltage relationships in the range −100 to +100 mV from a holding potential of 0 mV (inset in Fig. 1*A*). The currents flowing in response to these voltage ramps are plotted as a function of time. It is seen that after a short delay, an inwardly rectifying current develops as a consequence of the active depletion of intracellular calcium stores by $InsP_3$. Since I_{CRAC} is a voltage-independent calcium current with a reversal potential more positive than 0 mV, it is recorded as an inward current at 0 mV holding potential. The steady-state current flowing at 0 mV is shown in Fig. 1*B*. The shaded area at the beginning of the experiment corresponds to the time period in which the first twenty-seven short voltage ramps of Fig. 1*A* were applied. The spikes in Fig. 1*B* correspond to occasional sampling of unresolved currents evoked by the voltage ramps.

The fast activation of I_{CRAC} by $InsP_3$ was observed in 97% of the cells ($n = 560$) investigated under similar conditions as in Fig. 1. The extracellular application of ionomycin (14 μM) was similarly effective in inducing current activation (34 of 34 cells). The procedure of activating I_{CRAC} by perfusing mast cells with high concentrations of Ca^{2+} chelators was less reliable within the time span of a typical experiment (400 s). Under these conditions, calcium stores were not actively depleted but rather passively emptied by leakage of Ca^{2+} from the stores and, therefore, only 56% of the cells ($n = 66$) showed a noticeable calcium current which developed after a variable lag period (see Table 1).

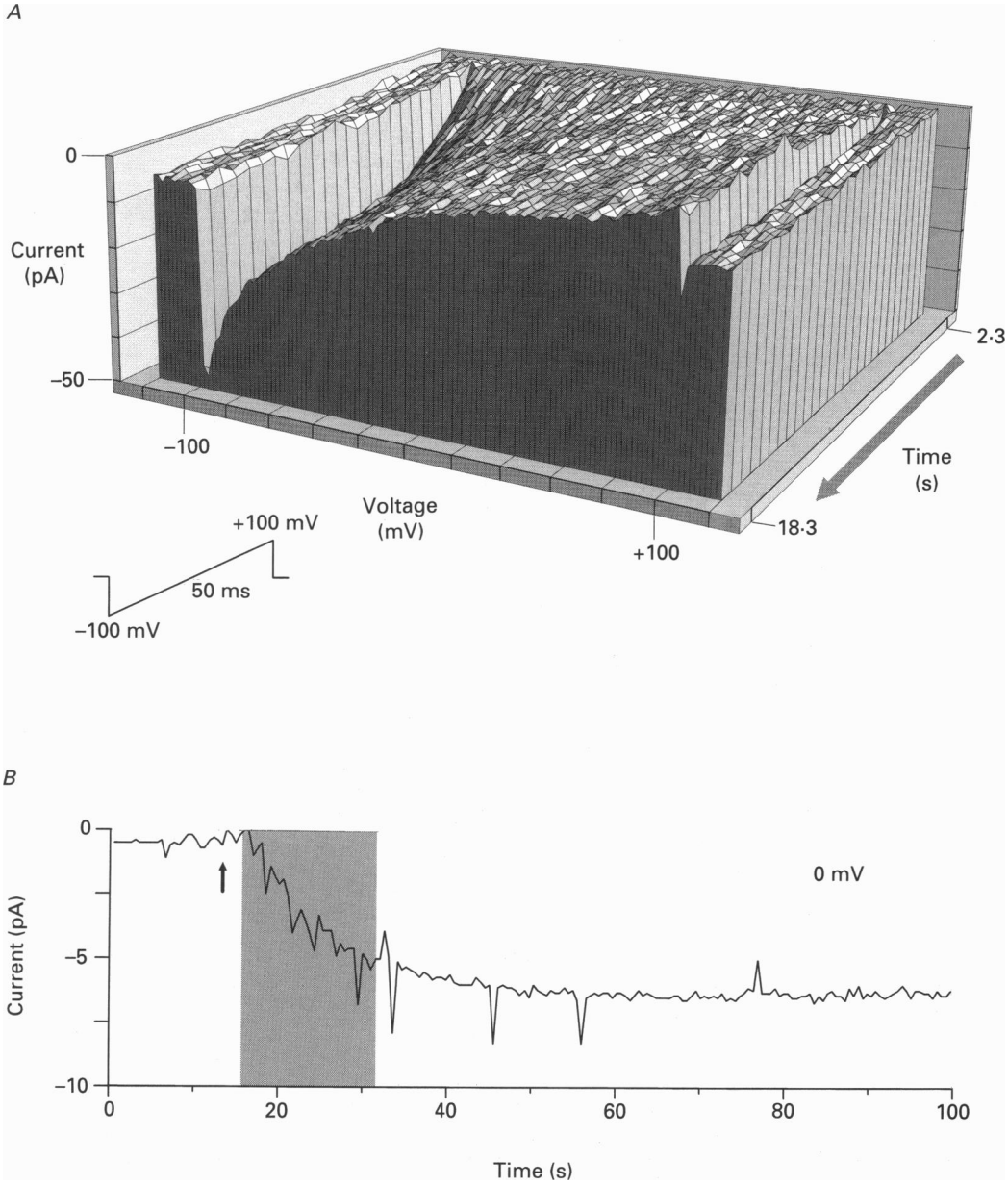

Fig. 1. Activation time course of I_{CRAC}. In this experiment, $InsP_3$ (10 μM) and EGTA (10 mM) were added to the standard pipette solution. Extracellular Ca^{2+} concentration was 10 mM. *A*, three-dimensional plot of high-resolution currents in response to the voltage-ramp protocol shown in the inset. Time progresses in direction of the arrow, with the first ramp current acquired 2·3 s after establishment of the whole-cell configuration. For clarity, only every fifth data point of the original sweeps (acquired at 10 kHz) were plotted. The first three ramps were pooled and subtracted as leak from all other sweeps. *B*, same experiment, showing the low-resolution current at the holding potential of 0 mV. The shaded area corresponds to the time period in which the ramps of *A* were acquired. The arrow indicates the time of establishing the whole-cell configuration.

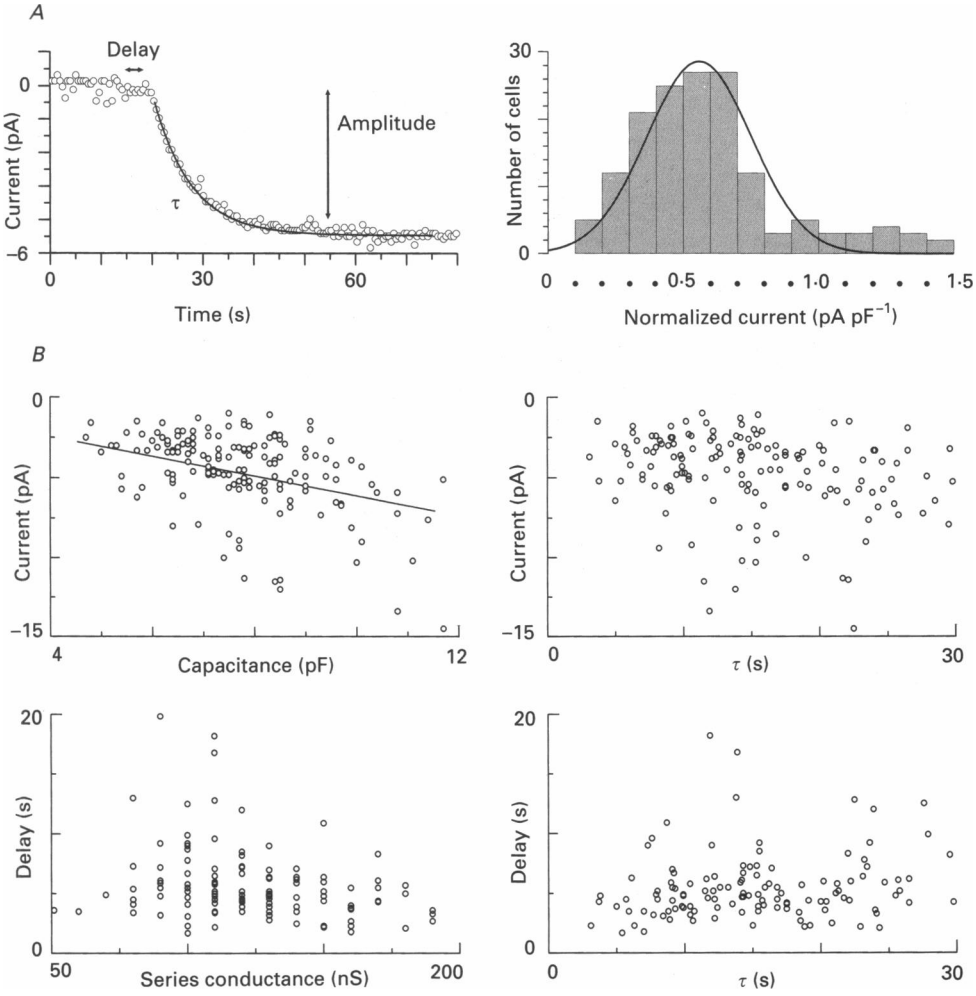

Fig. 2. Activation kinetics of I_{CRAC} and relationship to passive cell parameters. *A*, the left panel shows a typical time course of activation of I_{CRAC} at 0 mV (induced by 10 μM $InsP_3$ and 10 mM EGTA). It could be fitted by a single-exponential function, yielding the time constant (τ) and the current amplitude. The delay represents the time from break-in until activation of I_{CRAC}. The right panel shows the amplitude distribution of leak-corrected currents normalized to capacitance in 155 cells analysed this way. The distribution was fitted by a Gaussian fit according to $y = a\exp(-0{\cdot}5\,(x-b)/c)^2$, where x is the normalized current, y is the number of cells, a is the peak amplitude (29 cells), b is the mean current (0·57 pA pF^{-1}) and c is the half-width (0·19 pA pF^{-1}). *B*, plots of the various parameters (time constant, amplitude, delay, cell capacitance, and series conductance). Each data point corresponds to a single cell. Note the lack of correlation in all plots, except the relationship between capacitance and current, which was correlated as indicated by the linear regression line (slope = $-0{\cdot}6$ pA pF^{-1}, correlation coefficient = 0·31, $P = 0{\cdot}023$, t test).

Activation and inactivation kinetics of I_{CRAC}

Figure 2 shows the analysis of the kinetic parameters of I_{CRAC}. The activation time course can be fitted by a single-exponential function, yielding parameters of

amplitude and activation time constant τ. It is preceded by a delay, which reflects the time required for depleting the intracellular calcium stores and the activation steps involved in gating the plasma membrane conductance.

We analysed 160 experiments in which I_{CRAC} was activated by $InsP_3$ and EGTA. The current amplitudes were normalized to cell capacitance as a measure of surface

TABLE 1. Kinetic parameters of activation of I_{CRAC}

Pipette solutions (*external application)	Delay (s)	Time constant τ (s)	Current/capacitance (pA pF^{-1})
EGTA	192±33 (28)	44±10 (12)	−0·48±0·07 (12)
EGTA + $InsP_3$	6±1 (128)	18±1 (160)	−0·60±0·02 (160)
EGTA + *ionomycin	4±1 (5)	31±5 (10)	−0·52±0·05 (9)
BAPTA	306±40 (14)	46±16 (4)	−0·56±0·10 (4)
BAPTA + $InsP_3$	5±1 (10)	27±3 (13)	−1·10±0·13 (13)
BAPTA + *ionomycin	14±4 (8)	18±3 (7)	−1·03±0·16 (4)
Fura-2 + $InsP_3$	6±1 (11)	22±3 (11)	−0·61±0·08 (11)

Values represent means±S.E.M. (n) and were obtained by fitting a single exponential to the activation time course of I_{CRAC} under the specified conditions (holding potential was 0 mV). EGTA and BAPTA were employed at 10 mM, fura-2 was added at 2 mM, and $InsP_3$ was used at 10 μM. Ionomycin was applied extracellularly at 14 μM.

area, yielding an amplitude distribution of mean currents as shown in Fig. 2*A*. The amplitude distribution was fitted by a Gaussian function with a mean of 0·57±0·19 pA pF^{-} (±half-width), which corresponds to about 4·4 pA per cell, based on a mean mast cell capacitance of 7·8±0·1 pF (±S.E.M., n = 160). We have further analysed a possible correlation of the determined parameters (Fig. 2*B*). As expected, current amplitudes tended to increase in parallel with cell capacitance, indicating a constant current density with respect to membrane area. The delay to the activation of I_{CRAC} was largely independent of the series conductance, suggesting that the initial activation step involving depletion of calcium stores by infusion of $InsP_3$ was supramaximal and not limited by access resistance to the cytosol. Similarly, there was no correlation between the activation time constant and the measured delays or the current amplitudes (Fig. 2*B*), suggesting that the activation process follows an all-or-none behaviour and/or that there is an inherent rate-limiting step in the signal transduction process that is not imposed by the experimental conditions.

I_{CRAC} also developed spontaneously when adding EGTA or BAPTA (10 mM) to the pipette solution. This effect of the Ca^{2+} chelators is presumably due to the absorption of Ca^{2+} leaking from internal stores and preventing its reuptake, eventually causing depletion of calcium pools and activation of I_{CRAC}. Under these conditions, store depletion is passive and mainly depends on the leakiness of the stores. As a result, the delay before activation is considerably longer (see Table 1). The normalized current amplitude inducing passive store depletion by EGTA is not significantly different from experiments in which the calcium stores were actively depleted by $InsP_3$, whereas with BAPTA, current amplitudes were smaller than expected, considering the larger amplitudes seen in conjunction with active store depletion. The parameters for the activation of I_{CRAC} under various experimental conditions are summarized in Table 1.

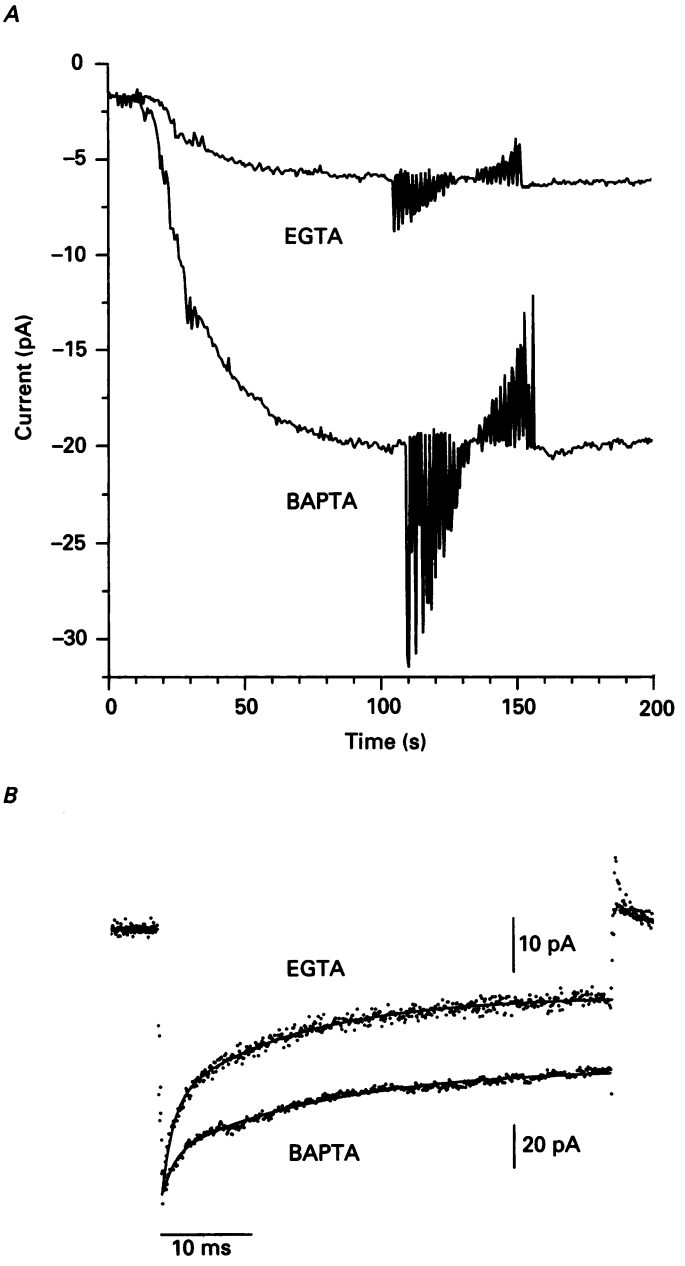

Fig. 3. Calcium-induced inactivation of I_{CRAC} with different Ca^{2+} buffers. *A*, superimposed low-resolution currents recorded at 0 mV after active depletion of Ca^{2+} stores by $InsP_3$ (10 μM) in the presence of EGTA or BAPTA (10 mM). At steady state, voltage steps to different potentials were applied (seen as unresolved current spikes). *B*, superimposed high-resolution currents elicited by hyperpolarizing voltage steps to -100 mV in the presence of EGTA and BAPTA, respectively. For comparison, the current sweep obtained with EGTA in the pipette was scaled to match the larger amplitude of the current under BAPTA. The continuous line is a double-exponential fit to the decay of the current according to $y = c + a_1 \exp(-t/\tau_1) + a_2 \exp(-t/\tau_2)$, where c is a constant corresponding

We asked whether I_{CRAC} is subject to Ca^{2+}-dependent inactivation by applying a short hyperpolarizing voltage pulse to -100 mV after I_{CRAC} had been activated by $InsP_3$ in the presence of EGTA or BAPTA (Fig. 3). In response to such a voltage step, there was an instantaneous increase in inward current which subsequently decreased by $64 \pm 3\%$ ($n = 3$) within 50 ms when EGTA (10 mM) was used as the intracellular buffer (Fig. 3*B*). When using the faster Ca^{2+} chelator BAPTA (10 mM) (Neher, 1986), the total whole-cell current was considerably larger than with EGTA (Fig. 3*A*, see also Table 1), while the decrease of the current amplitude in response to hyperpolarizing pulses was only $30 \pm 6\%$ ($n = 3$). We take this as evidence that the fast inactivation of I_{CRAC} is Ca^{2+} induced and that the lesser degree of fast inactivation and the larger whole-cell current amplitudes in the presence of BAPTA are due to its superior buffering kinetics as compared to EGTA.

Calcium dependence of I_{CRAC}

In the next series of experiments, we determined the dependence of the magnitude of I_{CRAC} on extracellular calcium concentration. This was done by relating the amplitudes of the current activated by $InsP_3$ in the presence of 10 mM external Ca^{2+} with those after varying the Ca^{2+} concentration (see Fig. 4*B*). The plot in Fig. 4*A* illustrates this relationship, showing the dependence of current amplitude of I_{CRAC} on the concentration of extracellular Ca^{2+}. The data could be approximated by a Michaelis–Menten function with an apparent dissociation constant (K_D) of 3·3 mM and a Hill coefficient of 1. The current was not completely abolished even at very low extracellular Ca^{2+} concentrations (< 10 μM). The remaining inward current measured about 6% of the steady-state amplitude obtained with 10 mM Ca^{2+} and may be due to monovalent cation fluxes.

Selectivity of I_{CRAC}

The current activated by releasing calcium from internal stores appears to primarily carry Ca^{2+} ions, since the reversal potential of I_{CRAC} is usually more positive than $+50$ mV and removal of Ca^{2+} from the bath solution almost completely abolishes the inwardly rectifying conductance (see Fig. 4). Reversal potential measurements of I_{CRAC} are compromised by its small amplitude and an occasional activation of a chloride conductance in mast cells (Matthews *et al.* 1989*b*). We have therefore used two alternative approaches to assess the specificity of I_{CRAC}. In the first type of measurement, we compared the selectivity of I_{CRAC} with that of a known voltage-activated calcium current in chromaffin cells (Fenwick, Marty & Neher, 1982*b*). This was achieved by using fura-2 as the dominant intracellular buffer (0·5–2 mM) and recording both changes in the Ca^{2+}-sensitive fluorescence (390 nm excitation wavelength) and Ca^{2+} currents in chromaffin cells and mast cells. Under these conditions, all incoming Ca^{2+} will be bound to fura-2 (Neher & Augustine, 1992)

---

to steady-state current after inactivation, a_1 and a_2 are amplitudes, τ_1 and τ_2 are time constants. The parameters for the experiments shown were: EGTA ($c = -17$ pA, $a_1 = -19$ pA, $a_2 = -16$ pA, $\tau_1 = 14$ ms, $\tau_2 = 1{\cdot}2$ ms); BAPTA ($c = -86$ pA, $a_1 = -42$ pA, $a_2 = -19$ pA, $\tau_1 = 18$ ms, $\tau_2 = 1{\cdot}2$ ms).

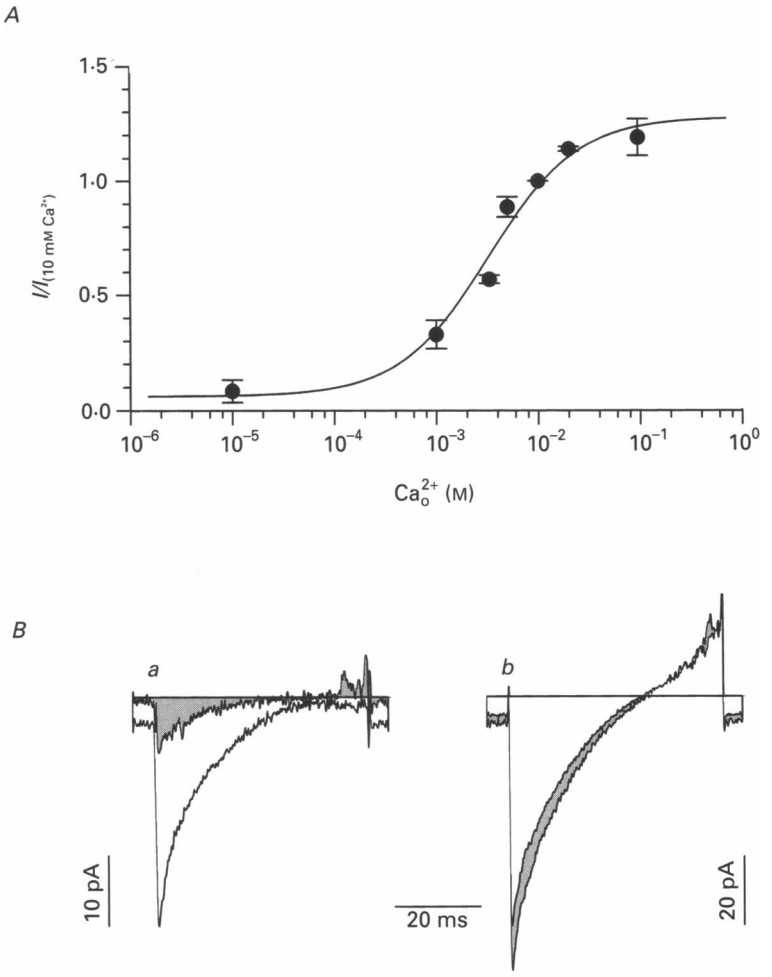

Fig. 4. Dependence of I_{CRAC} on extracellular Ca^{2+} concentration. *A*, 'dose–response' relationship for extracellular Ca^{2+} concentration. I_{CRAC} was activated by $InsP_3$ and EGTA in 10 mM extracellular Ca^{2+} and the desired test concentrations were applied from a puffer pipette. Data points correspond to the ratio of current amplitudes at −40 mV at various extracellular Ca^{2+} concentrations with respect to the standard Ca^{2+} concentration of 10 mM. The datum point with the lowest $[Ca^{2+}]_i$ was obtained in the presence of 1 mM EGTA with no Ca^{2+} added, and arbitrarily set to 10 μM (which we determined to be the free Ca^{2+} concentration of our Ringer solution in the absence of added Ca^{2+} and EGTA). Assigning the data point to lower $[Ca^{2+}]_o$ values did not affect the fitted curve. The curve was fitted according to $y = I_{min} + (I_{max}/(1 + (x/K_D)^n))$, where x is the extracellular Ca^{2+} concentration, y is the normalized current, I_{min} is the minimal current ratio (0·06), I_{max} is the maximal current ratio (1·21), K_D is the apparent dissociation constant (3·3 mM), and n is the Hill coefficient (1). The labels *a* and *b* next to the data points for 1 mM and 20 mM Ca^{2+} refer to the ramp-current traces shown in *B*. *B*, examples of high-resolution ramp currents, showing the effects of different extracellular Ca^{2+} concentrations on I_{CRAC}. The shaded ramp current was obtained after changing the extracellular Ca^{2+} concentration from 10 to 1 mM (*a*) and 20 mM (*b*), respectively.

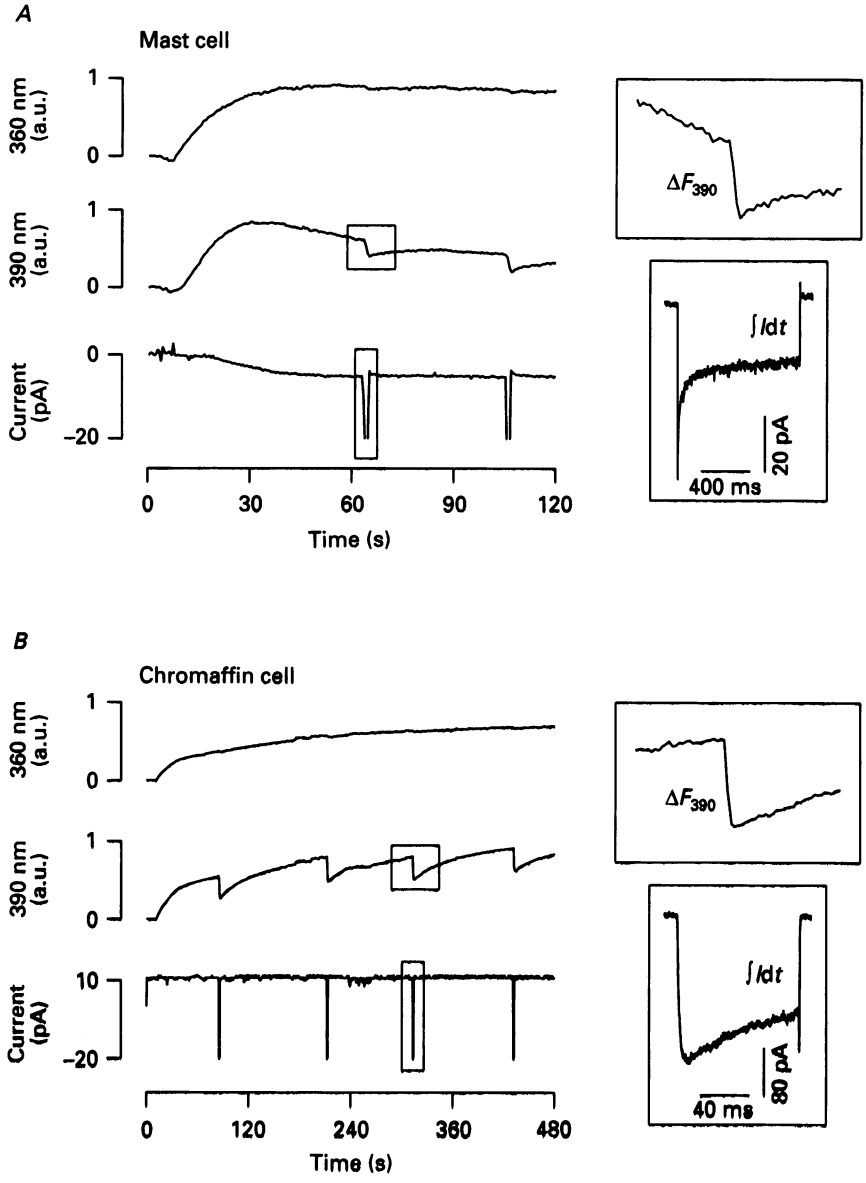

Fig. 5. Calcium fluxes through I_{CRAC} in mast cells and voltage-activated calcium currents in chromaffin cells. Effects of calcium currents on fura-2 fluorescence (360 and 390 nm) in mast cells (*A*) and chromaffin cells (*B*). Identical scalings apply to measured fluorescence values (in arbitrary units, a.u.) in both experiments, which were performed on the same experimental set-up on the same day. Shaded boxes in the low-resolution traces are magnified on the right, showing the change in the 390 nm signal and the inward current at higher resolution. *A*, I_{CRAC} was activated by $InsP_3$ (10 μM) and fura-2 was the only Ca^{2+} buffer added to the standard pipette solution (2 mM). Changes in fluorescence were recorded in response to hyperpolarizing voltage pulses (−100 mV) from the holding potential (0 mV), seen as truncated spikes in the low-resolution current trace. *B*, similar experiment to *A*, except that the pipette solution contained caesium glutamate instead of potassium glutamate and fura-2 was used at 0·5 mM. No $InsP_3$ was included in the

and together with the current integral this can be used to quantify the relative proportion of calcium that entered the cell during the current flow.

Figure 5 shows experiments performed under almost identical conditions in a chromaffin cell and a mast cell, the only major difference being the alternative ways of activating calcium influx. In both experiments fura-2 was loaded through the recording pipette into the cytosol. After loading was completed, calcium influx was induced either by a short depolarizing voltage pulse to open voltage-dependent calcium channels (Fig. 5*B*, chromaffin cell) or by a hyperpolarizing voltage pulse to increase the inward current through I_{CRAC}, which was previously activated by infusion of InsP_3 (Fig. 5*A*, mast cell). Both procedures induced an inward current which was accompanied by a decrease in the fura-2 fluorescence at 390 nm (see magnified insets in Fig. 5*A* and *B*). The absolute amount of fluorescence reduction (in arbitrary units) and the net charge transfer during the current flow (in pA s) can be quantified for both cell types by calculating the ratio (see Methods). The mean ratios were 63 ± 10 pA^{-1} s^{-1} ($n = 5$) for chromaffin cells and 79 ± 20 pA^{-1} s^{-1} ($n = 3$) for mast cells. If one compares these ratios, one arrives at an almost equivalent relative selectivity of 1 : 1·2 of voltage-dependent calcium currents in chromaffin cells and I_{CRAC} in mast cells, respectively.

Another way of determining the selectivity of I_{CRAC} for Ca^{2+} was performed by replacing extracellular Na^+ and K^+ with *N*-methyl-D-glucamine and leaving Ca^{2+} as the only charge carrier. Figure 6 shows that this resulted in a minor reduction of I_{CRAC} which on average was $9 \pm 2\%$ ($n = 4$), which compares favourably with the residual current observed after removal of extracellular Ca^{2+} in the reciprocal experiment (cf. Fig. 4) and further supports the notion that I_{CRAC} is highly selective for Ca^{2+} ions.

Blocking effects of divalent ions

A characteristic feature of calcium currents is that they are inhibited by other divalent ion species (Hille, 1992). We have tested for the blocking effects of various divalent cations on I_{CRAC}. Since these experiments were carried out in the presence of physiological Mg^{2+} concentrations (2 mM), we first investigated the effects of Mg^{2+} by varying its concentration in the external solution from 0 to 12 mM. Figure 7*A* illustrates the very minor effects on the amplitude of I_{CRAC} of changing the Mg^{2+} concentration from 2 to 0 and 10 mM, respectively. Figure 7*B* summarizes the actions of Mg^{2+} on I_{CRAC} and shows that the calcium current is well adapted to a wide range of extracellular Mg^{2+} concentrations.

Next we studied in some detail the blocking effects of Cd^{2+} and obtained a concentration–inhibition relationship for this ion as illustrated in Fig. 8*A*. The data points represent the percentage of inhibition as determined from ramp currents at −40 mV or currents in response to hyperpolarizing square pulses to −40 mV. Two examples for the inhibition of I_{CRAC} by different concentrations of Cd^{2+} (50 μM and 3 mM, respectively) are depicted in Fig. 8*B*. The block by Cd^{2+} was similarly effective

pipette solution and Na^+ and K^+ currents were blocked by TTX (1 μM) and TEA (10 mM). Calcium influx was induced by depolarizing voltage steps to +10 mV from a holding potential of −70 mV. See Methods and text for further details.

over the entire voltage range, suggesting a voltage-independent blocking mechanism. The data points could be adequately fitted by a Michaelis–Menten function, yielding an apparent K_D of 240 μM and a Hill coefficient of 1.

In order to establish a ranking order of potency for various other divalent ions, we chose to quantify the blocking efficacy of 1 mM of the respective divalent ion. We

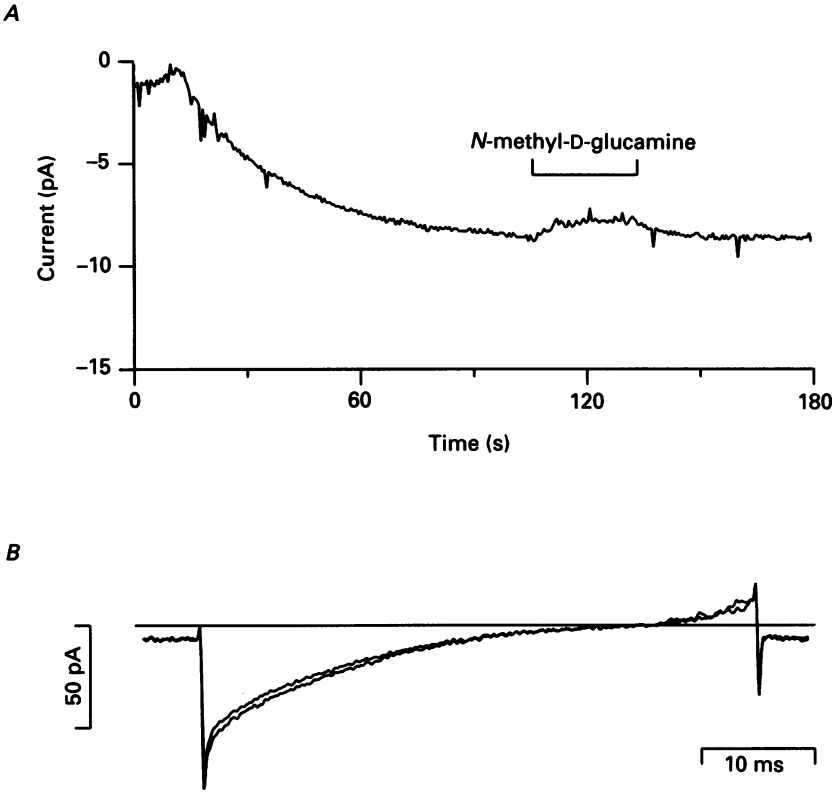

Fig. 6. Replacement of Na^+ and K^+ ions by *N*-methyl-D-glucamine. *A*, I_{CRAC} was activated by $InsP_3$ (10 μM) and BAPTA (10 mM). Low-resolution inward current at a holding potential of 0 mV. During the indicated time the standard extracellular bath solution was exchanged for a Ringer solution that maintained Ca^{2+} (10 mM), but in which Na^+ and K^+ were replaced by *N*-methyl-D-glucamine. *B*, superimposed high-resolution ramp currents (from −100 to +100 mV) in standard Ringer solution and in the *N*-methyl-D-glucamine-based solution.

found that all tested ions inhibited I_{CRAC} to variable degrees. Figure 9*A* shows the percentage of inhibition of I_{CRAC} by 1 mM of the respective ion species. Ba^{2+} and Sr^{2+}, which we found previously to be poorly permeant through I_{CRAC} (Hoth & Penner, 1992), are slightly inhibitory to currents carried by Ca^{2+}. Examples for small, moderate, and strong blocking effects of Ba^{2+}, Mn^{2+}, and Zn^{2+}, respectively are shown in Fig. 9*B* for both the current at 0 mV and for the full voltage range during a ramp.

La^{3+} is recognized as a potent blocker of Ca^{2+} influx. We found this trivalent ion

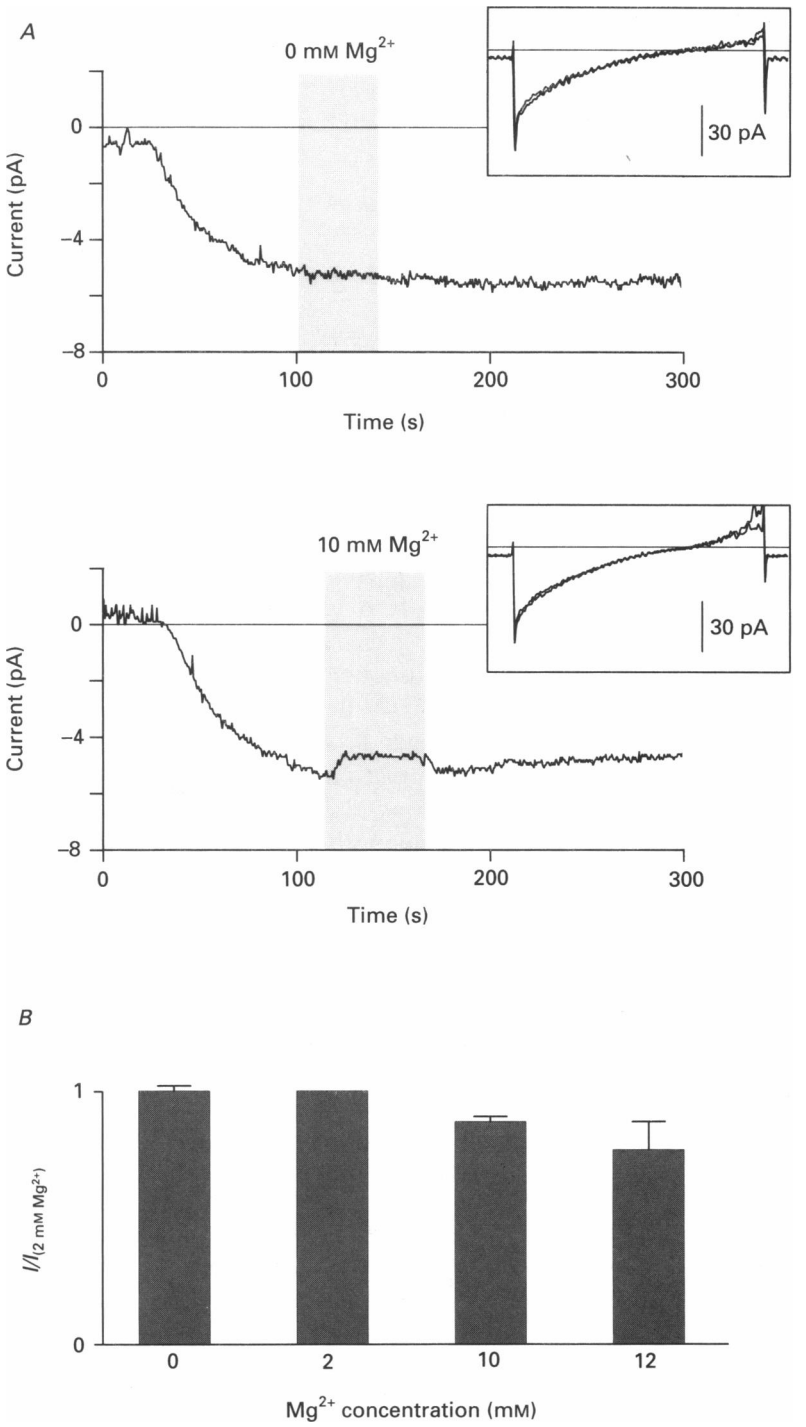

Fig. 7. Effects of extracellular Mg^{2+} concentration on I_{CRAC}. *A*, low-resolution current recordings (holding potential = 0 mV) and high-resolution ramp currents of I_{CRAC}, activated by InsP_3 (10 μM) and BAPTA (10 mM). During the indicated times, the standard

to be the most effective blocker of I_{CRAC}. Like with Zn^{2+}, there was a complete block of I_{CRAC} at 1 mM of La^{3+}. Comparing the blocking efficacy of the two ions at the lower concentration of 10 μM, yielded an average reduction of I_{CRAC} by Zn^{2+} of $24 \pm 4\%$ ($n = 3$) and by La^{3+} of $94 \pm 3\%$ ($n = 4$).

Permeation of monovalent ions

Voltage-activated calcium channels are known to lose their selectivity for Ca^{2+} ions in the absence of Ca^{2+} (Almers & McCleskey, 1984; Hess & Tsien, 1984). This phenomenon is also seen with I_{CRAC}, but only after complete removal of all divalent ions including Mg^{2+}. The effects of complete withdrawal of divalent ions from the extracellular solution and addition of EDTA (1 mM) to remove trace amounts of divalents are illustrated in Fig. 10. In this experiment, which is representative of eighteen cells, there was a triphasic change in the current characteristics. Panel *A* shows the membrane current at -40 mV and the currents in response to the standard voltage-ramp protocol are depicted in Fig. 10*B*. I_{CRAC} was activated by $InsP_3$ in the presence of 10 mM external Ca^{2+} and shows the typical inward rectification (*a*, seen in all 18 cells). When removing the divalents from the bath, there was an initial block of the inward current and a more pronounced outward component at positive potentials (*b*, resolved in 12 cells). We interpret this initial block to reflect the removal of Ca^{2+} as a charge carrier, while the residual Ca^{2+} ions impede the flow of monovalent ions. Subsequently, there was a sudden increase in inward current with moderate inward rectification and a shift in the reversal potential towards less positive potentials (*c*, seen in 17 cells). This current is presumably carried by Na^+ ions after complete removal of divalents. The increase in inward current was only transient and decayed within some 20–30 s, after which the whole-cell current had a rather linear behaviour over the entire voltage range with a reversal potential around 0 mV (*d*, observed in 13 cells). The decay of the monovalent current as well as the shift of the reversal potential to 0 mV could be due to an increase in intracellular Na^+, resulting in the gradual reduction of the driving force. In addition, there could be inhibitory actions of intracellular Na^+ on I_{CRAC}. Taken together, these results suggest that I_{CRAC} undergoes a transition from a calcium-selective to a non-selective cation current upon removal of divalent ions.

Variance analysis

As can be seen in Table 1, the whole-cell current carried by I_{CRAC} is rather small, even under optimal conditions (i.e. with high extracellular and low intracellular Ca^{2+} concentrations). The current was due to a conductance change, suggesting an ion channel mechanism, although it was not accompanied by detectable single-channel activity. We therefore attempted to use variance analysis to assess the single-channel conductance from the changes in current variance. An experiment that illustrates the

---

extracellular Mg^{2+} concentration was changed from 2 to 0 mM and 10 mM, respectively. *B*, mean relative changes in current amplitude at different extracellular Mg^{2+} concentrations with respect to the amplitude of I_{CRAC} in the presence of 2 mM Mg^{2+}. Error bars are $\pm$ S.E.M. ($n = 2$–7).

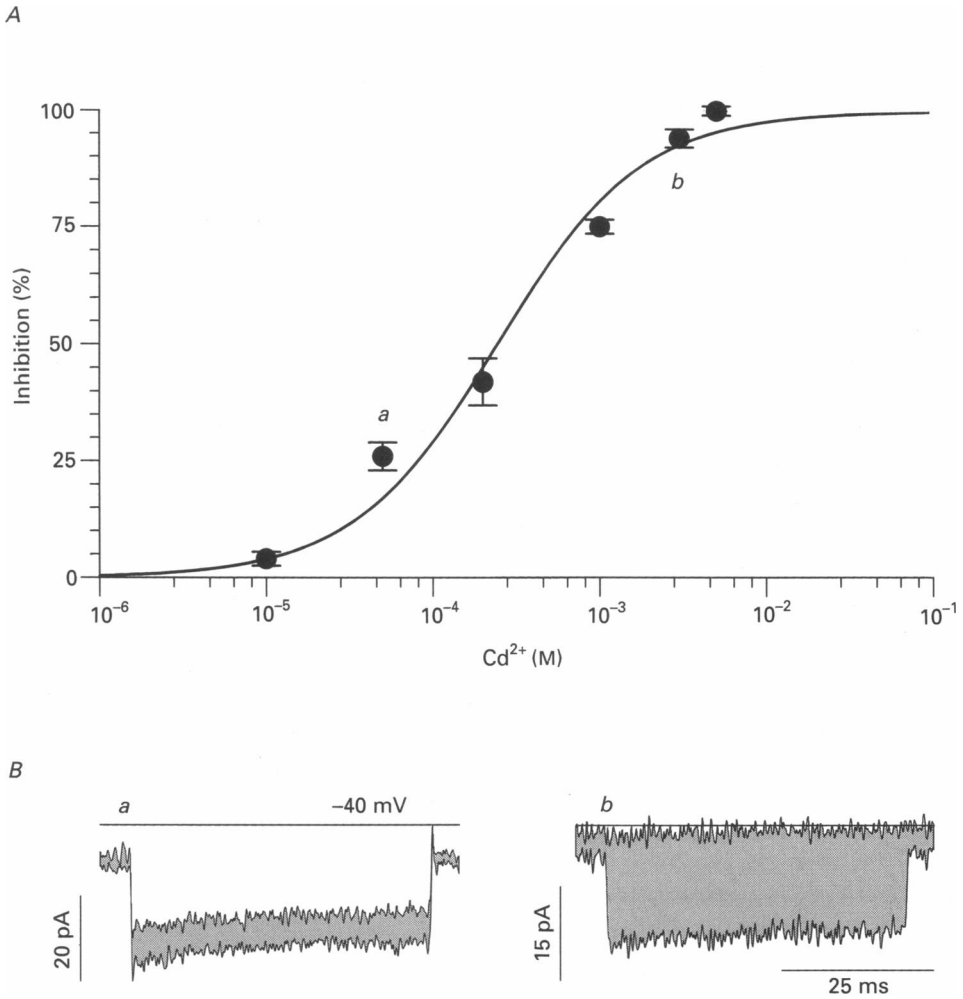

Fig. 8. Dose-dependent inhibition of I_{CRAC} by Cd^{2+}. *A*, 'dose–response' relationship for the inhibitory effects of extracellular Cd^{2+} concentration on I_{CRAC}. I_{CRAC} was activated by $InsP_3$ and EGTA in 10 mM extracellular Ca^{2+} and the desired test concentrations of Cd^{2+} were applied from a puffer pipette. Data points correspond to the inhibition of current amplitudes at −40 mV. The curve was fitted according to $y = 100/(1+(x/K_D)^n)$, where x is the external Cd^{2+} concentration, y is the inhibition, K_D is the apparent dissociation constant (240 μM), and n is the Hill coefficient (1). The labels *a* and *b* next to the data points for 50 μM and 3 mM Cd^{2+} refer to the current traces shown in *B*. *B*, examples of high-resolution currents in response to square voltage pulses to −40 mV, showing the effects of different extracellular Cd^{2+} concentrations on I_{CRAC}. The shaded area corresponds to the difference between currents acquired in the absence and the presence of 50 μM Cd^{2+} (*a*) and 3 mM Cd^{2+} (*b*), respectively.

changes in variance at different potentials before, during, and after activation of I_{CRAC} is shown in Fig. 11*A*. It is seen that the variance changes are extremely small and do not increase significantly after activation of I_{CRAC} by ionomycin.

Removal of divalent ions augments inward currents through I_{CRAC} (cf. Fig. 10). While this also caused an increase in current variance (Fig. 11*B*), this increase cannot

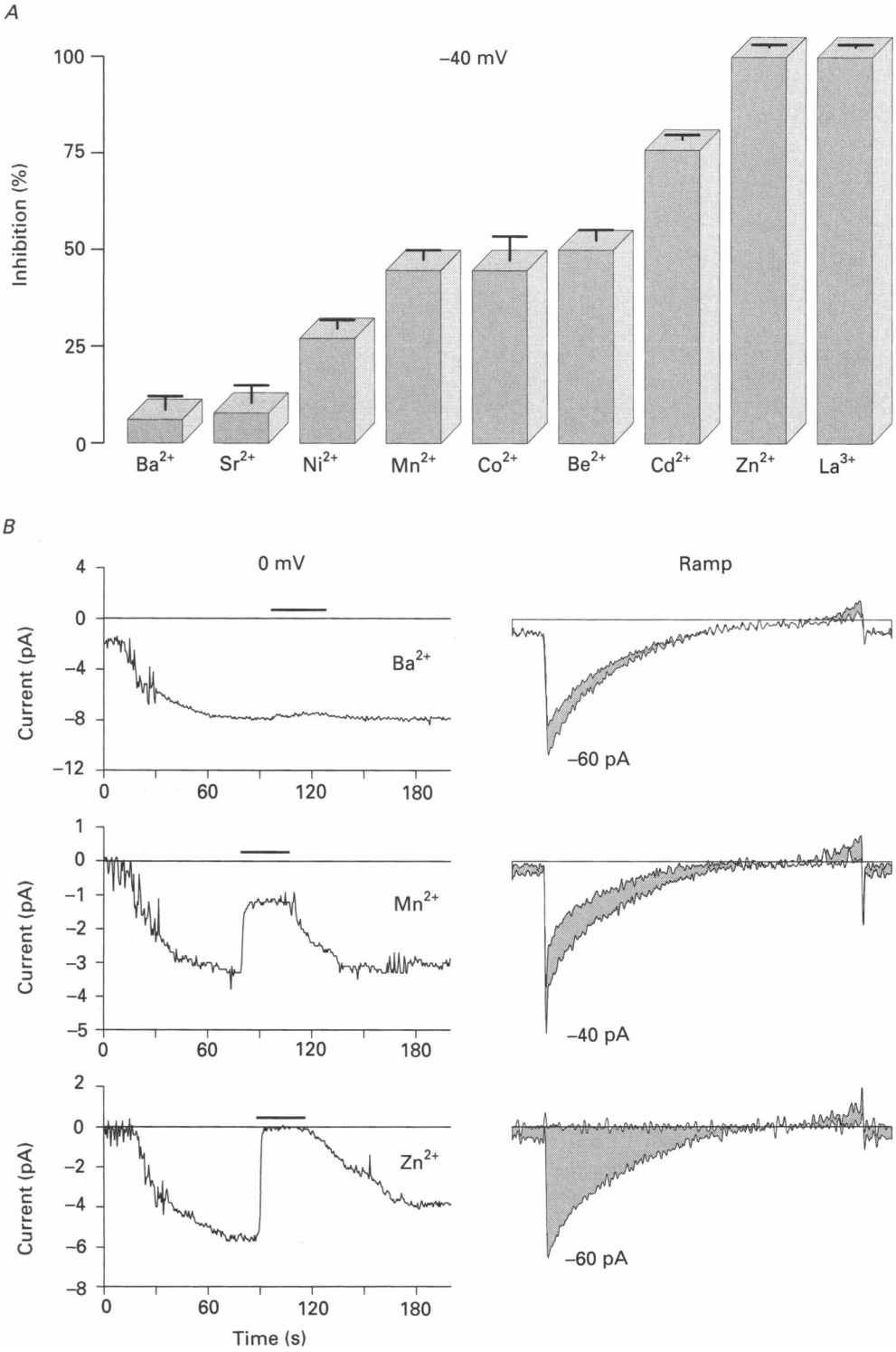

Fig. 9. For legend see facing page.

be utilized to assess the single-channel conductance, because upon changing the selectivity of I_{CRAC}, there is a concomitant shift in the reversal potential of the current. Variance analysis at more negative potentials is not feasible in mast cells, because the spontaneous activity of 50 pS cation channels (Matthews *et al.* 1989*a*) would mask a small variance change induced by I_{CRAC}. Nevertheless, this experiment suggests that the small increase in current noise reflects ion channel activity and that the single-channel conductance is likely to be well below 1 pS.

DISCUSSION

In this study, we have characterized the biophysical properties of the calcium current activated by depletion of intracellular calcium stores in mast cells. In particular, we have studied the kinetics and the selectivity of this current, the permeation of monovalent ions, and the blocking effects of divalent ions.

Kinetic properties of I_{CRAC}-active depletion

In our experiments, the activation of I_{CRAC} was usually induced by a high concentration of InsP_3 (10 μM) in order to obtain an instantaneous depletion of intracellular calcium stores. The K_D for InsP_3-induced calcium release as determined in microsomal preparations is in the submicromolar range (Meyer & Stryer, 1990). Therefore, we assume that under our conditions, the delivered concentration of InsP_3 was supramaximal and fully activated calcium release at the instant of achieving the whole-cell configuration. This is supported by the apparent independence of the delay of activation of I_{CRAC} from the measured series conductance, which determines the effective diffusional access of the pipette solution to the cytosol.

The delay before activation of the current (about 5–6 s) is presumably due to various, presently unknown steps involved in the signal transduction process that lead to the activation of I_{CRAC}. The initial triggering step is the depletion of InsP_3-sensitive stores. Fura-2 diffuses into the cell with a similar time course as InsP_3 and one can usually start to measure $[Ca^{2+}]_i$ reliably within 1–2 s after breaking into the cell. Typically, at this time, one can already see the falling phase of the InsP_3-induced Ca^{2+} transient, suggesting that the release process is rapid and probably completed within this period of time (Meyer & Stryer, 1990; Missiaen, De Smedt, Droogmans & Casteels, 1992). The fast onset of Ca^{2+} release by perfusing InsP_3 through patch pipettes is in agreement with studies in lacrimal gland cells, in which Ca^{2+} release was

Fig. 9. Blocking efficacy of various divalent ions. *A*, ranking order of the inhibition of I_{CRAC} by 1 mM of various divalent ions and the trivalent ion La^{3+}. I_{CRAC} was activated by InsP_3 and EGTA in 10 mM extracellular Ca^{2+} and the desired test concentrations of blocking ions were applied from a puffer pipette. Values represent means ± S.E.M. of 3 to 7 determinations and correspond to the inhibition of current amplitudes at −40 mV. *B*, examples of small (Ba^{2+}), moderate (Mn^{2+}), and strong (Zn^{2+}) inhibition of I_{CRAC}, activated by InsP_3 (10 μM) and EGTA (10 mM). Low-resolution current recordings of I_{CRAC} (holding potential = 0 mV) and high-resolution ramp currents. The desired blocking ions were added to the standard Ringer solution at 1 mM and were applied from a puffer pipette during the times indicated. The shaded area in the ramp currents corresponds to the difference between currents acquired before and during the application of the inhibitory ions, respectively.

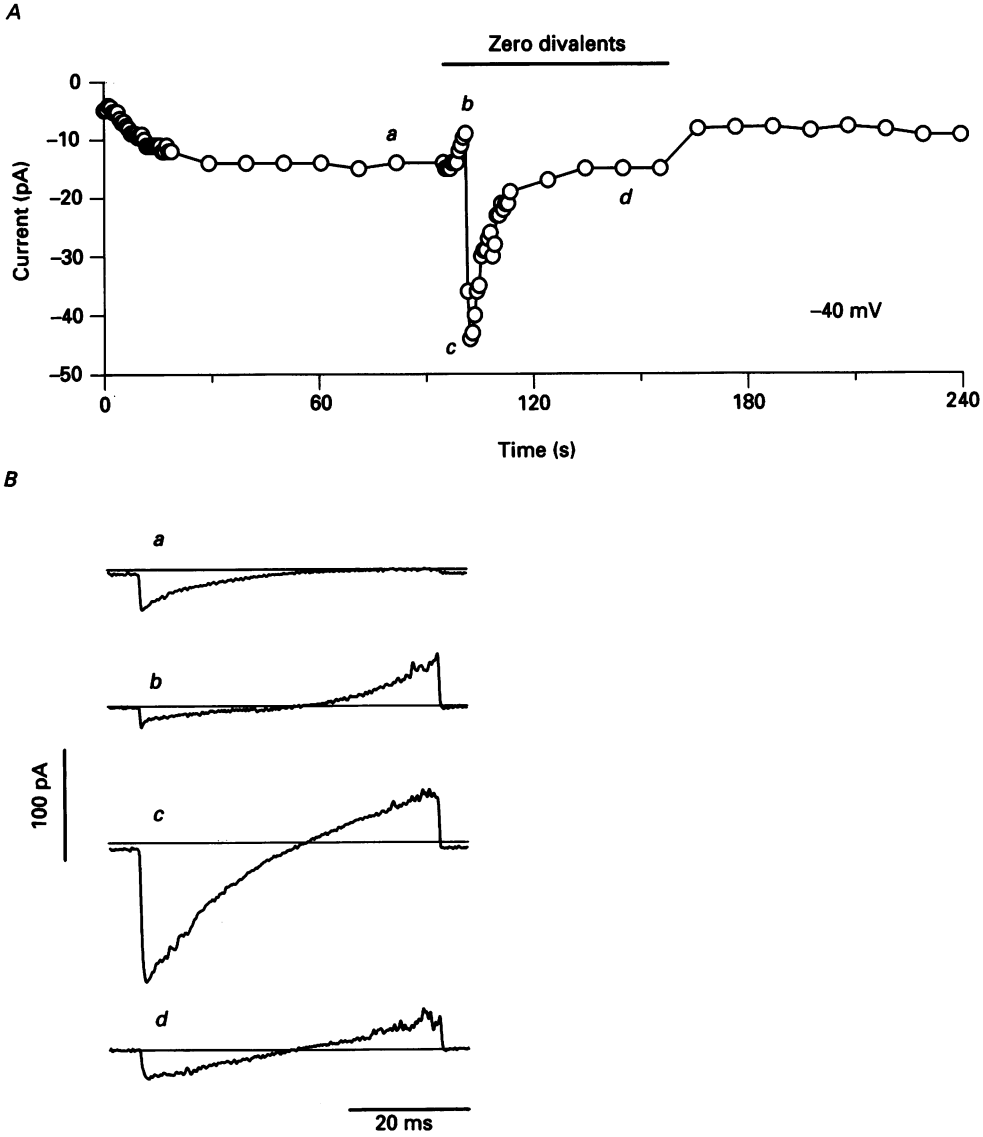

Fig. 10. Monovalent cation currents through I_{CRAC}. *A*, I_{CRAC} was activated by InsP_3 and EGTA in 10 mM extracellular Ca^{2+} at a holding potential of −40 mV. During the indicated time, the standard extracellular Ringer solution was replaced by a Ca^{2+}- and Mg^{2+}-free solution, supplemented by EDTA (1 mM) to chelate possible contaminations of divalent ions. The labels *a–d* next to the data points refer to the ramp-current traces shown in *B*. *B*, examples of high-resolution currents in response to voltage ramps. Points *a–d* show the various phases of the transition of I_{CRAC} from an inwardly rectifying Ca^{2+} current (with no clear reversal potential in this experiment) to a non-specific monovalent cation current with a reversal potential around 0 mV. See text for further details.

monitored indirectly by the recording of Ca^{2+}-activated chloride currents (Marty & Tan, 1989).

The other method used in this study to achieve an active depletion of calcium stores, was by applying the Ca^{2+} ionophore ionomycin. Ionomycin did not induce any

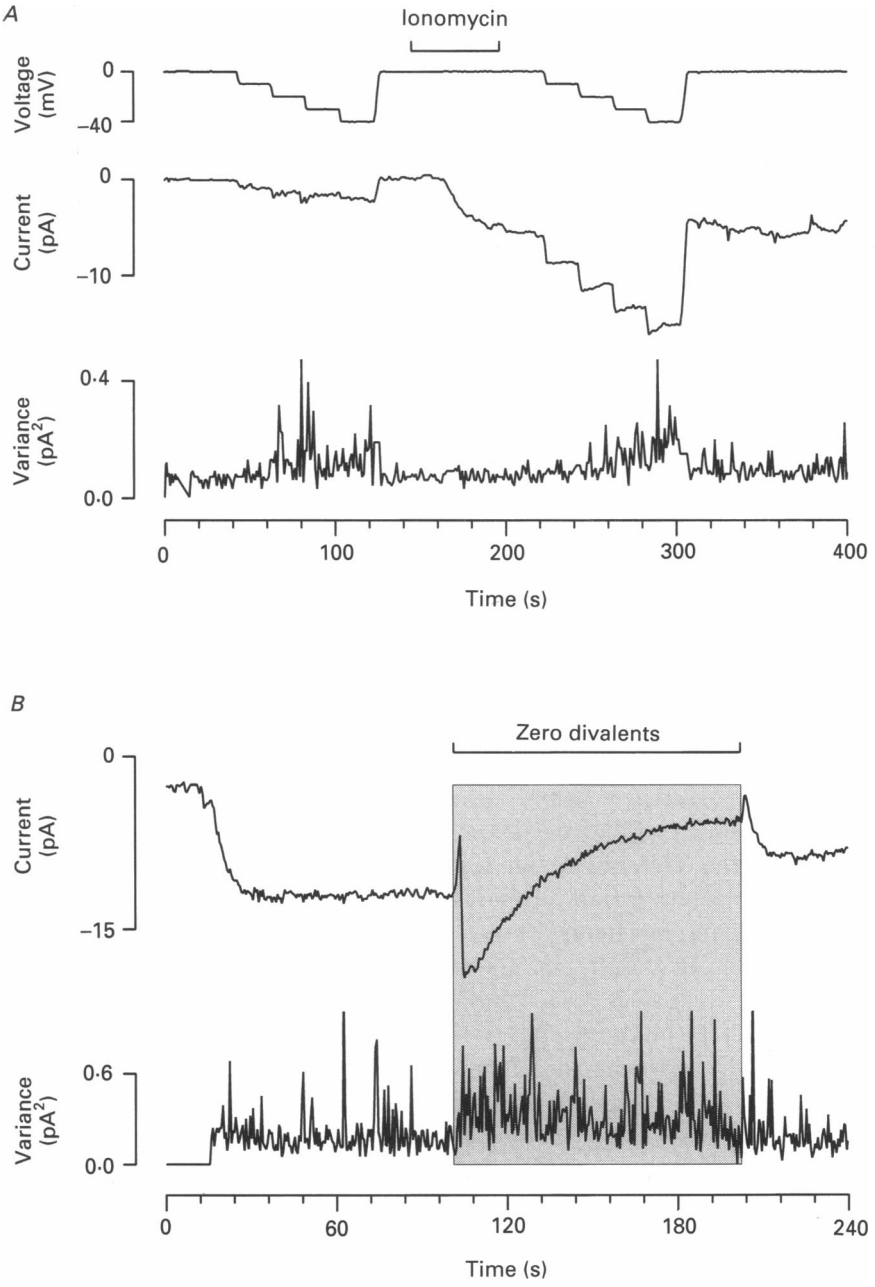

Fig. 11. Variance analysis of I_{CRAC}. *A*, changes in current and variance at various holding potentials before and after activation of I_{CRAC} by ionomycin (14 μM). Extracellular Ca^{2+} concentration was 10 mM throughout, while the pipette solution was supplemented with 10 mM EGTA. Note that there is no increase in current variance during activation of I_{CRAC}. Similarly, there was no significant change in the current noise at various potentials following application of ionomycin. *B*, similar experiment to *A*, except that I_{CRAC} was activated by $InsP_3$ (holding potential was 0 mV throughout) and extracellular Ringer solution was replaced by a divalent-free Ringer solution (1 mM EDTA added) as indicated. Note the slight increase in current variance during monovalent influx through I_{CRAC}. See Methods and text for further details.

current by itself, which conforms with the concept that it translocates Ca^{2+} across the plasma membrane by an electoneutral carrier mechanism (Liu & Hermann, 1978). Apparently, the ionophore not only affects the plasma membrane, but due to its lipophylic nature also reaches the calcium stores (Albert & Tashjian, 1986). It therefore constitutes a favourable tool to activate I_{CRAC} any time during an experiment. The parameters of ionomycin-induced calcium currents were not significantly different from the ones determined with active store depletion by $InsP_3$. Again, this suggests that the activation of I_{CRAC} is determined by the depletion of intracellular stores, regardless of the tool employed to achieve this.

The activation of the current was characterized by a single-exponential time course, largely independent of the activation mechanism used. There was no correlation of the activation time constant and the final current amplitude. This suggests that I_{CRAC} was activated supramaximally and that the mechanisms and steps involved in its activation appear to be homogeneous when using saturating $InsP_3$ concentrations. In most experiments, there was no or only a very small decay in the steady-state current within the typical duration of a measurement ($\sim$ 400–600 s). This may be due to the presence of Ca^{2+} buffers in our experiments which do not permit the refilling of Ca^{2+} stores after they have been depleted. Under more physiological conditions, calcium influx through I_{CRAC} will presumably inactivate after replenishment of empty stores. Occasionally, we have observed an inactivation of I_{CRAC} in experiments in which the amount of Ca^{2+} entering across the plasma membrane was unusually large and could not be coped with by the pipette-infused buffers. This manifested as an increase in $[Ca^{2+}]_i$ and a subsequent slow decrease of I_{CRAC} (M. Hoth & R. Penner, unpublished observation), that we consider mainly due to refilling of calcium stores, possibly supplemented by a component of calcium-dependent inactivation (as discussed below).

As evident from the voltage pulses to negative potentials, the initial inward current showed fast inactivation properties. This was probably not due to an inactivation of the gating mechanism by the refilling of stores, but rather to a Ca^{2+}-dependent inactivation of the ion channels themselves, since this inactivation was alleviated by BAPTA, which is a Ca^{2+} buffer with fast association kinetics (Neher, 1986). This action of Ca^{2+} may be effective only at high concentrations of Ca^{2+} and restricted to local domains near the channels. It thus appears that I_{CRAC} may be regulated through $[Ca^{2+}]_i$ by a mechanism equivalent to calcium-induced inactivation of voltage-activated Ca^{2+} channels (Eckert & Chad, 1984). At first sight, it may seem surprising that the normalized steady-state current amplitudes of I_{CRAC} measured at 0 mV holding potential were larger by a factor of two when BAPTA was used as Ca^{2+} chelator instead of EGTA. This may be accounted for by the same mechanism of Ca^{2+}-induced inactivation, since even at 0 mV there is still a considerable influx of Ca^{2+} due to the driving force provided by the concentration gradient of Ca^{2+} across the plasma membrane. This influx is sustained by a source of 10 mM extracellular Ca^{2+} and a sink provided by the intracellular Ca^{2+} buffer, which may generate locally a sufficiently high Ca^{2+} concentration at the cytoplasmic side of the plasma membrane to attenuate I_{CRAC} in the presence of EGTA, but to a lesser degree when using BAPTA.

Kinetic properties of I_{CRAC}-passive depletion

When activating I_{CRAC} by Ca^{2+} chelators, the delays are considerably longer, probably reflecting a passive depletion of calcium pools by leaks. The buffers then capture the Ca^{2+} in the cytosol and prevent its reuptake into the stores. This would result in the gradual depletion of the pools and eventually in the activation of I_{CRAC}. Interestingly, the normalized current amplitudes of I_{CRAC} induced by passive depletion with BAPTA were not bigger than with EGTA. This result is somewhat surprising, in view of the enhanced current amplitudes when BAPTA is used in conjunction with active store depletion. The basis for this difference remains unresolved and may point to uncertain side-effects of the two chelators. The time constants of activation of I_{CRAC} were slightly longer than the ones seen with active depletion of calcium stores by $InsP_3$, although this effect was not as pronounced as might have been expected from the long delays before activation of I_{CRAC}. One possible explanation for this virtually all-or-none behaviour of the activation process could reside in a high co-operativity of the mechanism that senses the calcium contents of the stores.

In analogy to the effects of intracellularly administered chelators, depletion of intracellular stores may also occur when removing extracellular calcium for extended periods, thus extracting intracellular Ca^{2+} into the extracellular medium. The ensuing activation of I_{CRAC} could be one mechanism for an enhanced influx of Ca^{2+} after readmission of calcium to the extracellular solution. The depletion of calcium stores by Ca^{2+} buffers is also analogous to the actions of thapsigargin, cyclopiazonic acid, and 2,5-di-tert-butylhydroquinone, all of which are thought to deplete the stores passively by interfering with Ca^{2+} uptake by pumps (Takemura, Hughes, Thastrup & Putney, 1989; Thastrup, Cullen, Drobak, Hanley & Dawson, 1990; Mason, Garcia-Rodriguez & Grinstein, 1991).

Calcium selectivity of I_{CRAC} and blocking effects of divalent ions

From several experimental approaches, we conclude that I_{CRAC} has an almost exclusive selectivity for Ca^{2+} ions, comparable to voltage-activated Ca^{2+} channels. First, the current is completely abolished by removal of extracellular Ca^{2+}. Second, most other divalent cations reduced I_{CRAC}. This includes Ba^{2+} and Sr^{2+}, which normally permeate effectively through voltage-dependent calcium channels (Almers & McCleskey, 1984; Hess & Tsien, 1984). However, we have noticed a complex behaviour of I_{CRAC} when replacing Ca^{2+} by Ba^{2+} ions. In some experiments we have observed an initial reduction and a subsequent slow increase in inward current with complex kinetics and complicated current–voltage relationship (M. Hoth & R. Penner, unpublished observations). Third, replacing Na^+ by *N*-methyl-D-glucamine did not significantly reduce I_{CRAC}, suggesting little if any permeation of monovalent ions. Only when all divalent ions are removed from the extracellular medium does the current lose its selectivity and become permeable to monovalent ions, a phenomenon that is also observed with voltage-activated calcium channels (Almers & McCleskey, 1984; Hess & Tsien, 1984). Fourth, the calcium selectivity of I_{CRAC} was comparable to the selectivity of voltage-dependent calcium currents in chromaffin cells when correlating the flux of Ca^{2+} by the charge movement across the membrane and the resulting fluorescence change of fura-2 in both cell types. Since the

permeability ratio of Ca^{2+} and Na^+ (P_{Ca}/P_{Na}) for voltage-activated Ca^{2+} channels is about 1000/1 (Hille, 1992), we assume a similarly high ratio for I_{CRAC}.

The activation of calcium influx through I_{CRAC} is the most effective way of raising $[Ca^{2+}]_i$ in mast cells and probably also in those cells in which this mechanism is present. The presence of a highly selective calcium current in mast cells has been postulated before, based on the correlation of extremely small whole-cell currents and changes in $[Ca^{2+}]_i$ following application of agonists and $InsP_3$ (Penner *et al.* 1988). The high selectivity of I_{CRAC} for Ca^{2+} and its sustained activation impose constraints on the cell-tolerable amplitude of the current, thereby preventing cytotoxic effects due to Ca^{2+} overload. Probably the small amplitude of this current under physiological conditions has hampered its detection in other cells in the past.

A rather selective Ca^{2+} current with similar current–voltage characteristics to I_{CRAC} but with oscillatory behaviour has been identified in lymphocytes (Lewis & Cahalan, 1989). This current developed spontaneously after establishment of the whole-cell configuration. In their report, Lewis & Cahalan have studied the Ca^{2+} current under conditions permissive for depletion of Ca^{2+} stores by using intracellular Ca^{2+} buffers (EGTA and BAPTA). In the light of the present study, the observed behaviour of the Ca^{2+} current in lymphocytes may have resulted from a cyclical depletion and refilling of intracellular stores.

Like other calcium-selective currents, I_{CRAC} was blocked by divalent metal ions. The relative potency of various divalents was assessed by applying them at 1 mM in the presence of 10 mM extracellular Ca^{2+}. The sequence of blocking efficacy is quite similar to the one found in smooth muscle cells (Murray & Kotlikoff, 1991) and rat basophilic leukaemia cells (RBL-2H3; Hide & Beaven, 1991). The surprising finding that Ba^{2+} and Sr^{2+} also reduced I_{CRAC} is quite different from the situation in voltage-dependent Ca^{2+} currents, where these ions do not block but permeate even better than Ca^{2+} does (Almers & McCleskey, 1984; Hess & Tsien, 1984). Probably, there is some permeation of Ba^{2+} and Sr^{2+} through I_{CRAC}, as reported by a change in the fluorescence properties of fura-2 (Hoth & Penner, 1992). The small blocking effects of these ions may arise from a small permeation through I_{CRAC} which then impedes the calcium flux.

There appears to be one major complication in relating I_{CRAC} to results obtained in other cell types. The current appears to exclude Mn^{2+}, which is often used to study Ca^{2+} influx induced by receptor stimulation or depletion of calcium stores (Jacob, 1990; Missiaen *et al.* 1990; Clementi, Scheer, Zacchetti, Fasolato, Pozzan & Meldolesi, 1992). The entry of Mn^{2+} can be monitored by a quench of fura-2 fluorescence. Under the conditions used in this and a previous study (Hoth & Penner, 1992), there was a block of I_{CRAC} and only a vanishingly small quench of fura-2 fluorescence by externally applied Mn^{2+}. This does not rule out a small permeation of Mn^{2+} through I_{CRAC}, which will probably remain undetected because of the high concentrations of intracellular buffers. BAPTA and EGTA will compete with fura-2 for Mn^{2+} and since they were used at much higher concentrations, preclude the binding of Mn^{2+} to the dye. Experiments designed to test for sources of Mn^{2+} influx have revealed that Mn^{2+} quenching of fura-2 can occur in mast cells under conditions that favour the activation of I_{CRAC} (C. Fasolato, M. Hoth & R. Penner, unpublished observation) and can also happen through receptor-activated non-selective cation

channels (C. Fasolato, M. Hoth, G. Matthews & R. Penner, unpublished observation).

Is I_{CRAC} an ion channel mechanism?

The current activated by depletion of intracellular Ca^{2+} stores was not associated with detectable single-channel activity. Nevertheless, several arguments support the notion that Ca^{2+} influx through I_{CRAC} is due to ion channels. The current was clearly due to a conductance change, since short hyperpolarizing voltage steps up to -200 mV produced an instantaneous, non-saturating current, which was characterized by Nernstian behaviour. Several other features such as the block by divalent metal ions and the permeation of monovalent ions in the absence of divalents are similar to voltage-activated Ca^{2+} channels and further support an ion channel hypothesis. However, the analysis of current variance showed that the changes in current noise are too small to be resolved in this cell type. This could be either due to an extremely small single-channel conductance of considerably less than 1 pS, or to the kinetic properties of the single channels, which would not flicker between open and closed states but may be characterized by long-lived open times.

Activation mechanisms of I_{CRAC}

It seems that the trigger for the activation of I_{CRAC} is provided by any mechanism that results in depletion of intracellular calcium stores. As a consequence of this depletion, there appears to be a mechanism that senses the Ca^{2+} content of the pools and generates a signal that induces the activation of I_{CRAC}. This signal has not been identified so far. At least three mechanisms appear conceivable: (1) a direct coupling of a membrane-spanning protein in the organelles that associates with the calcium channels in the plasma membrane; (2) a cognate mechanism through an enzymatic reaction such as phosphorylation or dephosphorylation of plasma membrane channels by organelle enzymes; (3) an indirect activation by an unidentified signalling molecule (a third messenger) generated by an unknown signal transduction cascade in the organelles.

For the first two mechanisms, there must be a close proximity of Ca^{2+} stores and the plasma membrane. There is evidence from a number of studies that in some cells there is an adjacent co-localization of the plasma membrane and parts of the endoplasmic reticulum (ER) (Rossier, Bird & Putney, 1991; McPherson, McPherson, Mathews, Campbell & Longo, 1992). The ER appears to act, at least in some cells, as a storage organelle for Ca^{2+} (Baumann, Walz, Somlyo & Somlyo, 1991). Other microsomal storage organelles (calciosomes) have been described (Volpe *et al.* 1988) but their localization needs further characterization. Recently, a microsomal fraction carrying $InsP_3$ binding properties has been shown to be associated with the plasma membrane (Rossier *et al.* 1991) and disaggregated by cytochalasin, a treatment that interferes with cytoskeletal elements.

A direct protein–protein interaction appears as an intriguing mechanism for signal transduction between organelles and plasma membrane, particularly in view of a closely related mechanism found in skeletal muscle that operates in the reverse direction. There, the mechanism of excitation–contraction coupling is thought to involve a plasma membrane protein (the dihydropyridine receptor, a putative

calcium channel) that activates a calcium release channel of organelles (the ryanodine receptor in the sarcoplasmic reticulum) through a protein–protein interaction. It has been suggested that in non-muscle cells this physical coupling mechanism is provided by the InsP_3 receptor in the storage organelles and the inositol 1,3,4,5-tetrakisphosphate (InsP_4) receptor in the plasma membrane (Irvine, 1990). However, we have so far been unable to find any effect of InsP_4 on Ca^{2+} influx in mast cells. In addition, I_{CRAC} appears to be activated under conditions in which neither InsP_3 nor InsP_4 are expected to be generated.

A similarly tight activation mechanism could involve an enzymatic transduction mechanism provided by organelle-associated enzymes that modify the plasma membrane channels. This may be accomplished by phosphorylation or dephosphorylation of the channels by kinases or phosphatases associated with the calcium stores. Although there is little known about the modulation of Ca^{2+} influx in non-excitable cells, the fact that voltage-activated calcium channels are modulated by phosphorylation reactions (Kameyama, Hescheler, Hofmann & Trautwein, 1986) would not render this possibility unlikely.

A less tight and stringent mechanism of activation may be operational through the generation of a signalling messenger released from the calcium stores upon depletion of Ca^{2+}. Such a mechanism, involving cytochrome P450 or one of its metabolites, has been proposed based on the inhibitory effects on Mn^{2+} entry of substances that inhibit microsomal cytochrome P450 (Alvarez, Montero & Garcia-Sancho, 1992). However, the same substances also appear to inhibit voltage-activated Ca^{2+} influx (Villalobos, Fonteriz, Lopez, Garcia & Garcia-Sancho, 1992), which are not gated by depletion of Ca^{2+} stores. Our data do not add much evidence to decide which of the possible mechanisms may be responsible for the activation of Ca^{2+} influx through I_{CRAC}. Based on the finding that there was a persistent activation of I_{CRAC} for minutes in the whole-cell configuration, in which the cytosol is constantly and effectively dialysed, one should be surprised if the conductive state of the channels was controlled by a constant supply of a diffusible 'third' messenger.

We thank M. Pilot for technical assistance. This work was supported in part by the Deutsche Forschungsgemeinschaft (grant 243/3-1), the Sonderforschungsbereich 236, and the Hermann- und Lilly-Schilling-Stiftung.

REFERENCES

ALBERT, P. R. & TASHJIAN, A. H. (1986). Ionomycin acts as an ionophore to release TRH-regulated Ca^{2+} stores from GH_4C_1 cells. *American Journal of Physiology* **251**, C887–891.

ALMERS, W. & MCCLESKEY, E. W. (1984). Non-selective conductance in calcium channels of frog muscle: calcium selectivity in a single-file pore. *Journal of Physiology* **353**, 585–608.

ALVAREZ, J., MONTERO, M. & GARCIA-SANCHO, J. (1992). Cytochrome P450 may regulate plasma membrane Ca^{2+} permeability according to the filling state of the intracellular Ca^{2+} stores. *FASEB Journal* **6**, 786–792.

BAUMANN, O., WALZ, B., SOMLYO, A. V. & SOMLYO, A. P. (1991). Electron probe microanalysis of calcium release and magnesium uptake by endoplasmic reticulum in bee photoreceptors. *Proceedings of the National Academy of Sciences of the USA* **88**, 741–744.

BERRIDGE, M. J. & IRVINE, R. F. (1989). Inositol phosphates and cell signalling. *Nature* **341**, 197–205.

CLEMENTI, E., SCHEER, H., ZACCHETTI, D., FASOLATO, C., POZZAN, T. & MELDOLESI, J. (1992). Receptor-activated Ca^{2+} influx. *Journal of Biological Chemistry* **267**, 2164–2172.

ECKERT, R. & CHAD, J. E. (1984). Inactivation of Ca channels. *Progress in Biophysics and Molecular Biology* **44**, 215–267.

FENWICK, E. M., MARTY, A. & NEHER, E. (1982*a*). A patch-clamp study of bovine chromaffin cells and of their sensitivity to acetylcholine. *Journal of Physiology* **331**, 577–597.

FENWICK, E. M., MARTY, A. & NEHER, E. (1982*b*). Sodium and calcium channels in bovine chromaffin cells. *Journal of Physiology* **331**, 599–635.

HESS, P. & TSIEN, R. W. (1984). Mechanism of ion permeation through calcium channels. *Nature* **309**, 453–456.

HIDE, M. & BEAVEN, M. A. (1991). Calcium influx in a rat mast cell (RBL-2H3) line. *Journal of Biological Chemistry* **266**, 15221–15229.

HILLE, B. (1992). *Ionic Channels of Excitable Membranes*. Sinauer, Sunderland, MA, USA.

HOTH, M. & PENNER, R. (1992). Depletion of intracellular calcium stores activates a calcium current in mast cells. *Nature* **355**, 353–356.

IRVINE, R. F. (1990). 'Quantal' Ca^{2+} release and the control of Ca^{2+} entry by inositol phosphates – a possible mechanism. *FEBS Letters* **263**, 5–9.

JACOB, R. (1990). Agonist-stimulated divalent cation entry into single cultured human umbilical vein endothelial cells. *Journal of Physiology* **421**, 55–77.

KAMEYAMA, M., HESCHELER, J., HOFMANN, F. & TRAUTWEIN, W. (1986). Modulation of Ca current during the phosphorylation cycle in the guinea pig heart. *Pflügers Archiv* **407**, 123–128.

LEWIS, R. & CAHALAN, M. D. (1989). Mitogen-induced oscillations of cytosolic Ca^{2+} and transmembrane Ca^{2+} current in human leukemic T cells. *Cell Regulation* **1**, 99–112.

LIU, C. & HERMANN, T. E. (1978). Characterization of ionomycin as a calcium ionophore. *Journal of Biological Chemistry* **253**, 5892–5894.

MCPHERSON, S. M., MCPHERSON, P. S., MATHEWS, L., CAMPBELL, K. P. & LONGO, F. J. (1992). Cortical localization of a calcium release channel in sea urchin eggs. *Journal of Cell Biology* **116**, 1111–1121.

MAHAUT-SMITH, M. P., SAGE, S. O. & RINK, T. J. (1992). Rapid ADP-evoked currents in human platelets recorded with the nystatin permeabilized patch technique. *Journal of Biological Chemistry* **267**, 3060–3065.

MARTY, A. & TAN, Y. P. (1989). The initiation of calcium release following muscarinic stimulation in rat lacrimal glands. *Journal of Physiology* **419**, 665–687.

MASON, M. J., GARCIA-RODRIGUEZ, C. & GRINSTEIN, S. (1991). Coupling between intracellular Ca^{2+} stores and the Ca^{2+} permeability of the plasma membrane. *Journal of Biological Chemistry* **266**, 20856–20862.

MATTHEWS, G., NEHER, E. & PENNER, R. (1989*a*). Second messenger-activated calcium influx in rat peritoneal mast cells. *Journal of Physiology* **418**, 105–130.

MATTHEWS, G., NEHER, E. & PENNER, R. (1989*b*). Chloride conductance activated by external agonists and internal messengers in rat peritoneal mast cells. *Journal of Physiology* **418**, 131–144.

MELDOLESI, J., CLEMENTI, E., FASOLATO, C., ZACCHETTI, D. & POZZAN, T. (1991). Ca^{2+} influx following receptor activation. *Trends in Pharmacological Sciences* **12**, 289–292.

MELDOLESI, J. & POZZAN, T. (1987). Pathways of Ca^{2+} influx at the plasma membrane: voltage-, receptor-, and second messenger-operated channels. *Experimental Cell Research* **171**, 271–283.

MEYER, T. & STRYER, L. (1990). Transient culture release induced by successive increments of inositol 1,4,5-trisphosphate. *Proceedings of the National Academy of Sciences of the USA* **87**, 3841–3845.

MISSIAEN, L., DECLERCK, I., DROOGMANS, G., PLESSERS, L., DE SMEDT, H., RAEYMAEKERS, L. & CASTEELS, R. (1990). Agonist-dependent Ca^{2+} and Mn^{2+} entry dependent on state of filling of Ca^{2+} stores in aortic smooth muscle cells of the rat. *Journal of Physiology* **427**, 171–186.

MISSIAEN, L., DE SMEDT, H., DROOGMANS, G. & CASTEELS, R. (1992). Ca^{2+} release induced by inositol 1,4,5-trisphosphate is a steady-state phenomenon controlled by luminal Ca^{2+} in permeabilized cells. *Nature* **357**, 599–602.

MURRAY, R. K. & KOTLIKOFF, M. I. (1991). Receptor-activated calcium influx in human airway smooth muscle cells. *Journal of Physiology* **435**, 123–144.

NEHER, E. (1986). Concentration profiles of intracellular calcium in the presence of a diffusible chelator. *Experimental Brain Research* **14**, 80–96.

NEHER, E. (1989). Combined fura-2 and patch clamp measurements in rat peritoneal mast cells. In *Neuromuscular Junction*, ed. SELLIN, L. C., LIBELIUS, R. & THESLEFF, S., pp. 65–76. Elsevier, Amsterdam.

NEHER, E. & AUGUSTINE, G. J. (1992). Calcium gradients and buffers in bovine chromaffin cells. *Journal of Physiology* **450**, 273–301.

PENNER, R., MATTHEWS, G. & NEHER, E. (1988). Regulation of calcium influx by second messengers in rat mast cells. *Nature* **334**, 499–504.

PUTNEY, J. W. (1990). Capacitative calcium entry revisited. *Cell Calcium* **11**, 611–624.

ROSSIER, M. F., BIRD, G. S. & PUTNEY, J. W. (1991). Subcellular distribution of the calcium-storing inositol 1,4,5-trisphosphate-sensitive organelle in rat liver. Possible linkage to the plasma membrane through the actin microfilaments. *Biochemical Journal* **274**, 643–650.

SAGE, S. O. (1992). Three routes for receptor-mediated Ca^{2+} entry. *Current Biology* **2**, 312–314.

TAKEMURA, H., HUGHES, A. R., THASTRUP, O. & PUTNEY, J. W. (1989). Activation of calcium entry by the tumor promoter thapsigargin in parotid acinar cells. *Journal of Biological Chemistry* **264**, 12266–12271.

THASTRUP, O., CULLEN, P. J., DROBAK, B. K., HANLEY, M. R. & DAWSON, A. P. (1990). Thapsigargin, a tumor promoter, discharges intracellular Ca^{2+} stores by specific inhibition of the endoplasmic reticulum Ca^{2+} ATP-ase. *Proceedings of the National Academy of Sciences of the USA* **87**, 2466–2470.

VILLALOBOS, C., FONTERIZ, R., LOPEZ, M. G., GARCIA, A. G. & GARCIA-SANCHO, J. (1992). Inhibition of voltage-gated Ca^{2+} entry into GH_3 and chromaffin cells by imidazole antimyotics and other cytochrome P450 blockers. *FASEB Journal* **6**, 2742–2747.

VOLPE, P., KRAUSE, K.-H., HASHIMOTO, S., ZORZATO, F., POZZAN, T., MELDOLESI, J. & LEW, D. P. (1988). 'Calciosome', a cytoplasmic organelle: the inositol 1,4,5-trisphosphate-sensitive Ca^{2+} store of nonmuscle cells? *Proceedings of the National Academy of Sciences of the USA* **85**, 1091–1095.

VON ZUR MÜHLEN, F., ECKSTEIN, F. & PENNER, R. (1991). Guanosine 5′-[β-thio]triphosphate selectively activates calcium signalling in mast cells. *Proceedings of the National Academy of Sciences of the USA* **88**, 926–930.